Characterization of amylose inclusion complexes using electron paramagnetic resonance spectroscopy

Lingyan Kong – University of Alabama
Umut Yucel – Kansas State University
Rangrong Yoksan – Kasetsart University
Ryan J. Elias – Pennsylvania State University
Gregory R. Ziegler – Pennsylvania State University

Citation of published version:

Kong, L., Yucel, U., Yoksan, R., Elias, R., Ziegler, G. (2018): Characterization of amylose inclusion complexes using electron paramagnetic resonance spectroscopy. *Food Hydrocolloids*, vol. 82.

DOI: https://doi.org/10.1016/j.foodhyd.2018.03.050

Full text at https://doi.org/10.1016/j.foodhyd.2018.03.050
or send request to lingyan.kong@ua.edu

Characterization of Amylose Inclusion Complexes Using Electron Paramagnetic Resonance Spectroscopy

Lingyan Kong[a], Umut Yucel[b], Rangrong Yoksan[c], Ryan J. Elias[d], and Gregory R. Ziegler[d,*]

[a] Department of Human Nutrition and Hospitality Management, The University of Alabama, Tuscaloosa, AL 35487, USA

[b] Department of Animal Sciences and Industry, Kansas State University, Manhattan, KS 66506, USA

[c] Department of Packaging and Materials Technology, Faculty of Agro-Industry, Kasetsart University, Bangkok 10900, Thailand

[d] Department of Food Science, The Pennsylvania State University, University Park, PA 16802, USA

[*]Corresponding author. Tel.: (814)863-2960; fax: (814)863-6132. Address: 341 Rodney A. Erickson Food Science Building, University Park, PA 16802, USA

E-mail address: grz1@psu.edu

ABSTRACT

Amylose is well known to form inclusion complexes with various small molecules including fatty acids. In this study, we prepared amylose inclusion complexes with stearic acid derived spin probes and demonstrated the electron paramagnetic resonance (EPR) spectroscopy as an emerging tool for studying the microstructure and microenvironment of amylose-guest inclusion complex. Two spin probes, namely 5-doxyl-stearic acid (5-DSA) and 16-doxyl-stearic acid (16-DSA), were used as guest molecules in forming amylose-guest inclusion complexes. The molecular dynamics and local polarity of the spin probes and their interaction with amylose in physical mixtures and inclusion complexes were studied using EPR spectroscopy. Complexed guest spin probes could be released when the inclusion complex was dissolved dimethyl sulfoxide (DMSO) and detected by EPR. Since the inclusion complex could not be dissolved in water, the motion of spin probes was restricted in hydrated samples shown by the powder-like slow spectra. Our findings also indicated that the individual association between amylose and the two DSA molecules in forming the inclusion complexes were different. A portion of 16-DSA molecules were not tightly immobilized in the amylose helical channel, but instead were loosely entrapped in the amorphous region of the semicrystalline V_6-type amylose. Therefore, EPR spectroscopy provides valuable information on the molecular dynamics and microenvironment of guest molecules and their interaction with amylose in inclusion complex, and can be exploited as a useful tool to study amylose-guest inclusion complex and other host-guest systems.

Keywords: Amylose; Doxyl-stearic acid; Inclusion complex; Electron paramagnetic resonance (EPR); Molecular dynamics

1. Introduction

Amylose, the essentially linear component of the starch polymer, is known to form inclusion complexes with a number of small molecules, such as iodine (Bluhm & Zugenmaier, 1981; Immel & Lichtenthaler, 2000), alcohols (Whittam et al., 1989), aroma compounds (Conde-Petit, Escher, & Nuessli, 2006; Tapanapunnitikul, Chaiseri, Peterson, & Thompson, 2007), and fatty acids and their esters (Biliaderis, Page, Slade, & Sirett, 1985; Kong & Ziegler, 2014a, 2014b; Lay Ma, Floros, & Ziegler, 2011; Lesmes, Cohen, Shener, & Shimoni, 2009). In the presence of small guest molecules, e.g., iodine and fatty acids, the amylose forms six-fold, left-handed single helices that may crystallize in an antiparallel arrangement known as the V_6 or V_h (V-hydrate) type amylose, with a hexagonal unit cell structure (parameters a = b = 13.65 Å, c = 8.05 Å) (Brisson, Chanzy, & Winter, 1991). The ability of amylose to form inclusion complexes with small molecules has a profound influence on the quality attributes of nearly all starch-containing foods. For example, the formation of inclusion complexes with either native or added lipids can dramatically influence the pasting properties of starch, retard starch retrogradation, and extend the shelf life of baked goods (Eliasson & Wahlgren, 2004; Stauffer, 1995). The structure of amylose-fatty acids inclusion complexes has been intensively studied by X-ray diffraction (XRD) (Godet, Buleon, Tran, & Colonna, 1993; Le Bail et al., 1999), nuclear magnetic resonance (NMR) (Lebail, Buleon, Shiftan, & Marchessault, 2000), and differential scanning calorimetry (DSC) (Biliaderis, Page, & Maurice, 1986; Karkalas, Ma, Morrison, & Pethrick, 1995), and to some extent small-angle X-ray scattering (SAXS) (Putseys, Gommes, Van Puyvelde, Delcour, & Goderis, 2011), transmission electron microscopy (TEM) (Godet, Bouchet, Colonna, Gallant, & Buleon, 1996), and Raman spectroscopy (Carlson, Larsson, Dinh‐Nguyen, & Krog, 1979). However, the molecular interactions between fatty acids and

amylose molecules, as well as the localization and orientation of the guest fatty acids within the amylose single helices, have not been completely elucidated.

Electron paramagnetic resonance (EPR) is a technique to study the microenvironments of biological systems, such as lipid bilayers (Deo, Somasundaran, Subramanyan, & Ananthapadmanabhan, 2002; Garay & Rodrigues, 2008), membranes (Štrancar, Šentjurc, & Schara, 2000), as well as physicochemical systems, such as micelles (Brigati, Franchi, Lucarini, Pedulli, & Valgimigli, 2002), vesicles (Bratt & Kevan, 1993; Deo & Somasundaran, 2002; Nakagawa, 2009), microemulsions (Avramiotis, Cazianis, & Xenakis, 2000; Kristl, Volk, Gašperlin, Šentjurc, & Jurkovič, 2003), liposomes (Kristl et al., 2003), self-assembling polymer systems (Beghein et al., 2007), organic nanochannels (Barbon, Zoleo, Brustolon, Comotti, & Sozzani, 2008), and inclusion complexes (Bardelang et al., 2006; Mezzina, Cruciani, Pedulli, & Lucarini, 2007). EPR can provide important information about molecular dynamics and local polarity of spin probes within these systems. Certain spin probes, especially those derived from fatty acids, may thus be used to study the interaction between amylose and fatty acids in forming inclusion complexes. For example, 5- and 16-doxyl-stearic acids (5-DSA and 16-DSA) (Fig. 1a and b) are derivatives of stearic acid and carry a doxyl ring moiety containing a nitroxide radical, which make them EPR-active.

Only a few studies employed the EPR technique to study the interaction between starch and EPR-active radicals (i.e., spin probes), yet no effort was made to intentionally create amylose-guest inclusion complexes. Spin probes 5- and 16-DSA were added into aqueous dispersions of different types of starch (e.g., wheat, potato, corn, high amylose corn, and waxy corn starch) during heating and cooling (Biliaderis & Vaughan, 1987; Nolan, Faubion, & Hoseney, 1986; Pearce, Davis, Gordon, & Miller, 1985, 1987; Wasserman & Le Meste, 2000; Windle, 1985), with the main purpose of following the gelatinization and recrystallization of starch. These researchers did notice more restricted motion of 5- and 16-

DSA in starch dispersions, as compared to spin probes without fatty acid moiety, including 2,2,6,6-tetramethylpiperidine-1-oxyl (TEMPO) (Nolan et al., 1986; Pearce et al., 1985), 4-Hydroxy-TEMPO (Wasserman & Le Meste, 2000), and 4-(2-bromoacetamido)-TEMPO (Biliaderis & Vaughan, 1987). Similar behavior was observed when using other fatty acid derived spin probes, e.g., methyl 5-DSA (Pearce et al., 1987) and TEMPO-laurate (Nolan et al., 1986). However, the strong binding of the fatty acid derived spin probes shown by EPR spectra was more likely to be due to the adsorption or immobilization of the spin probes on starch molecules, instead of the formation of inclusion complex. The transition between rapid and slow motion of the 5-DSA and 16-DSA was reversible during heating and cooling around the temperature range that coincides with the gelatinization of starch, not the dissociation of inclusion complex (Wasserman & Le Meste, 2000). The spectra prior to heating and after cooling from 65 °C, 95 °C, and 125 °C showed little noticeable difference in shape and the calculated hyperfine extrema separation, which is used to describe spectra changes in slow motion (Pearce et al., 1987; Wasserman & Le Meste, 2000). It suggested that this type of strong binding exists before heating and thus before inclusion complexation could take place. However, the available evidence was not sufficient to fully exclude the possibility of inclusion complex induced slow motion. The inclusion complex formation, if any, was not addressed by other complementary techniques such as XRD and DSC in these studies.

Hence, in the present work, we focused on the preparation of amylose-x-DSA inclusion complexes and their characterization by complementary XRD, DSC, FTIR, and EPR techniques. Their behavior was also compared to the that of the non-complex forming spin probe, 4-phenyl-2,2,5,5-tetramethyl-3-imidazoline-1-oxyl nitroxide (PTMIO) (Figure 1c). The molecular dynamics of spin probes and their physical mixtures and inclusion complexes with amylose were studied by EPR spectroscopy, in order to investigate the degree of

rotational mobility and probe environment, and to understand the molecular interactions between x-DSA and amylose molecules.

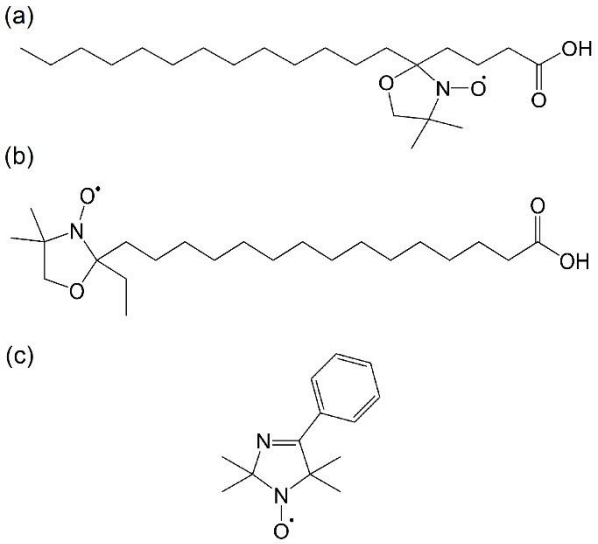

Fig. 1. Chemical structures of (a) 5-doxyl-stearic acid (5-DSA), (b) 16-doxyl-stearic acid (16-DSA), and (c) 4-Phenyl-2,2,5,5-tetramethyl-3-imidazoline-1-oxyl nitroxide (PTMIO).

2. Materials and Methods

2.1. Materials

Amylose (Type III, from potato, essentially free of amylopectin), 5-doxyl-stearic acid (5-DSA), 16-doxyl-stearic acid (16-DSA), and 4-Phenyl-2,2,5,5-tetramethyl-3-imidazoline-1-oxyl nitroxide (PTMIO) were purchased from Sigma-Aldrich Inc. (St. Louis, MO). Dimethyl sulfoxide (DMSO) was supplied by VWR International (Radnor, PA). Potassium bromide (KBr) powder was obtained from Thermo Fisher Scientific (Waltham, MA).

2.2. Preparation of amylose inclusion complexes

Amylose (100 mg) was dissolved in 2mL of 95% (v/v) aqueous DMSO by stirring at 90 °C for 30 min. Guest compound (5 mg), i.e., spin probe, was added and then the mixture was vigorously stirred for 2 min using a vortex stirrer. The mixture was held at 90 °C for 30 min,

diluted with 5 mL of deionized water at 90 °C, and held for an additional 15 min before being allowed to cool to room temperature (20 °C) overnight. The precipitate was collected by centrifugation (Allegra^{TM} 6, Beckman Coulter, Indianapolis, IN) at 3000 g for 10 min, washed 3 times with 50% (v/v) aqueous ethanol, and dried in a hot air oven (VWR, Radnor, PA) at 45 °C for 3 h.

2.3. Wide angle X-ray diffraction

Wide angle X-ray diffraction (XRD) patterns were obtained using a Rigaku MiniFlex II desktop X-ray diffractometer (Rigaku Americas Corporation, TX). The dry powders were equilibrated over saturated KCl at 20 °C (R.H. 85%) for at least 24 h prior to XRD analysis. Samples were exposed to Cu Kα radiation (0.154 nm) and continuously scanned between 2θ = 4 and 30 ° at a scanning rate of 1 °/min with a step size of 0.02 °. A current of 15 mA and voltage of 30 kV were used. Data were analyzed using the Jade v.8 software (Material Data Inc., Livermore, CA).

2.4. Differential scanning calorimetry

Approximately 5 to 6 mg of sample was weighed into a 60 µL stainless steel pan (Perkin-Elmer Instruments, Norwalk, CT) and deionized water added to obtain a 20% (w/v) suspension. The pan was hermetically sealed and equilibrated at room temperature (20 °C) for at least 3 h. The samples were equilibrated to 10 °C, and then heated to 180 °C at a heating rate of 5 °C/min in a Thermal Advantage Q100 differential scanning calorimetry (DSC, TA Instruments, New Castle, DE). The DSC was calibrated with indium, and an empty sample pan was used as the reference. Data was analyzed using the TA Universal Analysis software (Universal Analysis 2000 v.4.2E, TA Instruments, New Castle, DE).

157 *2.5. Fourier transform infrared spectroscopy*

158 Dry powders (1%, w/w) were rigorously mixed with KBr for 30 s, and pressed into a
159 transparent pellet using a pellet maker. Spectra were obtained using a Research Series Galaxy
160 3020 Fourier transform infrared (FTIR) spectrometer (Madison Instrument, Inc., Middleton,
161 WI) in transmission mode over the wave number range of 400 – 4000 cm^{-1}, with an
162 accumulation of 16 scans and a resolution of 4 cm^{-1}.

163 *2.6. Electron paramagnetic resonance (EPR)*

164 Electron paramagnetic resonance (EPR) measurements of spin probes (100 μM), and their
165 physical mixtures containing 100 μM of spin probes, and inclusion complex samples were
166 conducted using a Bruker eScanR spectrometer (Bruker BioSpin, Billerica, MA) operating in
167 X-band at room temperature (20 °C). The EPR spectra were recorded with a minimum
168 resolution of 0.1 G at a microwave frequency of 9.78 GHz, a microwave power of 18.97 mW,
169 and a modulation amplitude of 0.98 G. Samples were deoxygenated by passing nitrogen (0.5
170 L/min) through the samples for about 10 – 15 min, then loaded into 100 μL glass capillary
171 tubes (VWR, International, Inc., Radnor, PA), and sealed with Critoseal® (McCormick
172 Scientific, St. Louis, MO) prior to EPR measurements.

173 Two types of spectra were obtained: fast-tumbling spectra of the radicals in solutions
174 (rotational correlation time lower than 1 ns), and slow tumbling spectra of immobilized
175 radicals. The solution spectra (i.e., in the fast motion regime) were simulated, and rotational
176 correlation times (τ_c ; inversely related to mobility), signal intensity (I; double integration of
177 the characteristic first derivative EPR signal), and hyperfine splitting constants (A_0; function
178 of the polarity of the environment for a given spin-probe) were quantified using the
179 WinSim2002 software (version 0.98, National Institute of Environmental Health Sciences,
180 National Institutes of Health, USA), and as described in (Yucel, Elias, & Coupland, 2012).

For slow spectra, for example the amylose-5-DSA inclusion complex hydrate (Fig. S1 in Supplementary Materials), the change in the mobility can be evaluated from the change in the separation of the outermost peaks ($A_{||}$) as compared to that in the rigid (i.e., dry powder) spectra ($A_{\perp}$) (Freed, 1976; Wu & Gaffney, 2006). A rotational correlation time can be calculated by assuming Brownian diffusion model as:

$$\tau_c = (0.54ns)\left(1 - \frac{A_{||}}{A_{max}}\right)^{-1.36} \quad [1]$$

where $A_{max} = A_{||}$ in rigid spectra, and $2A_{||}$ is the separation of the outermost peaks (Fig. S1 in Supplementary Materials). The effect of motion about the long axis on the axial averaging (i.e., a measure of the extent of probe immobilization) can be evaluated by an arbitrary order parameter, S, defined as follows (Gaffney, 1976; Griffith & Jost, 1976):

$$S = \frac{A_{||} - A_{\perp}}{A_{max} - A_{min}} \quad [2]$$

where $A_{min} = A_{\perp}$ in the rigid spectra (Fig. S1 in Supplementary Materials). The order parameter, S, is the extent of probe immobilized, but is also affected by the heterogeneity of the motion (Freed, 1976; Gaffney, 1976).

EPR spectra were measured in triplicates. Quantitative data were presented as mean ± standard deviation (SD). One-way ANOVA was conducted and $p < 0.05$ indicated significant difference.

3. Results and Discussion

3.1. Formation of amylose-x-DSA inclusion complexes

The products obtained by precipitating amylose and x-DSA from hot aqueous dimethyl sulfoxide (DMSO) displayed X-ray diffraction (XRD) peaks at 2θ of ca. 13.5 and 20.5 ° (Fig. 2A), which are characteristic of V_6-type amylose-guest inclusion complex (Godet et al.,

1993). It suggests that the spin probe molecules, i.e., 5-DSA and 16-DSA, are able to induce inclusion complexation with amylose, where they are trapped within the cavity of the amylose single helices. As a comparison, the raw amylose without any complexed agent was largely amorphous (Fig. 2). Without guest molecules capable of inducing amylose inclusion complexation, no inclusion complex could precipitate. The PTMIO molecule is too bulky to be accommodated in the helical channel of the V_6-type amylose, the diameter of which is about 5.4 Å (Immel & Lichtenthaler, 2000). On the other hand, the linear alkyl chains of fatty acids and their esters possesses the right size, shape and hydrophobicity to fit into the V_6-type amylose channel, as demonstrated by a number of researchers (Kong & Ziegler, 2014a, 2014b; Lay Ma et al., 2011; Lorentz et al., 2012). In this study, the substitution of the doxyl group on the alkyl chain of stearic acid and its location on either C5 or C16 did not seem to affect their ability to form inclusion complexes with amylose. In 5-DSA, the nitroxide moiety is close to the lipid polar head, leaving an apolar alkyl tail of 13 carbons long, whereas in 16-DSA, the nitroxide moiety and the hydroxyl group are on the opposite ends of an alkyl chain consisting of 14 carbons. The linear alkyl chains of the x-DSA were thus responsible for inducing inclusion complexation with amylose, despite the bulky nitroxide moiety and its position on C5 or C16.

The thermal properties of the amylose-x-DSA inclusion complex samples were examined by a differential scanning calorimeter (DSC). The amylose-5-DSA and amylose-16-DSA samples exhibited endotherms with peak temperatures at 94 and 101 °C, respectively (Fig. 2). The endotherms were attributed to the dissociation of amylose-x-DSA inclusion complexes. According to the Safety Data Sheets provided by the supplier (Sigma-Aldrich, Inc.), the melting points of 5-DSA and 16-DSA are 51-53 °C and 47-55 °C, respectively. Therefore, the endotherms seen at temperatures above 90 °C were not due to the melting of the spin probes. Without a complexing agent, amylose would not show any noticeable endotherm

below approximately 120 °C during heating. The thermal stability of amylose-fatty acid inclusion complexes was found to increase with fatty acid chain length (Tufvesson, Wahlgren, & Eliasson, 2003). Given the longer linear alkyl chain of 16-DSA than 5-DSA, its inclusion complex correspondingly showed higher thermal stability. Overall, the endothermic peak temperatures of amylose-x-DSA were close to those of amylose inclusion complexes with fatty acids of 12 to 16 carbons (Karkalas et al., 1995; Tufvesson et al., 2003).

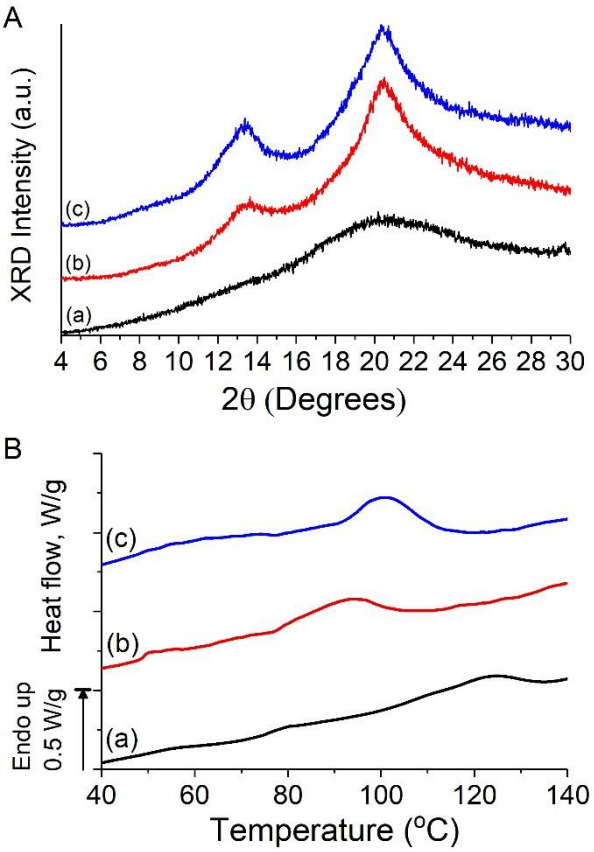

Fig. 2. (A) XRD patterns and (B) DSC thermograms of (a) raw amylose, (b) amylose-5-DSA inclusion complex and (c) amylose-16-DSA inclusion complex.

Both 5-DSA and 16-DSA showed characteristic bands in FTIR spectra at about 2850 and 1710 cm^{-1} (Fig. 3), which were assigned to the CH_2 stretching of the alkyl chain and carbonyl stretching, respectively (Kong & Ziegler, 2014a) and absent in the amylose spectrum. These bands appear in amylose-x-DSA inclusion complex samples (Fig. 3d and e), indicating the

presence of x-DSA. Therefore, complementary XRD, DSC, and FTIR techniques together provide evidence that the x-DSA molecules were encapsulated in the amylose inclusion complexes.

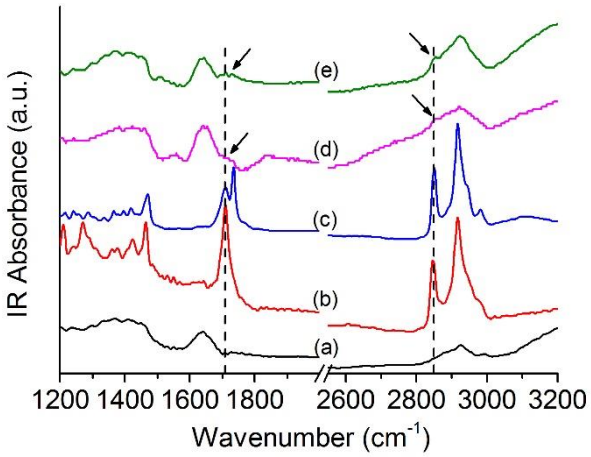

Fig. 3. FTIR spectra of (a) amylose, (b) 5-DSA, (c) 16-DSA, (d) amylose-5-DSA inclusion complex and (e) amylose-16-DSA inclusion complex.

3.2. EPR study of amylose-x-DSA inclusion complexes

The EPR spectra of all spin-probes in DMSO and water were, as expected, the characteristic triplet (Fig. 4A & B). The signal intensities decreased when water was used as medium for x-DSA. The EPR spectra of amylose and x-DSA physical mixtures in DMSO showed slightly decreased amplitude (Fig. 4C), indicating lower mobility in the presence of amylose. The presence of amylose might increase the microviscosity experienced by the spin probes, but did not induce any strong immobilization in the DMSO medium where amylose remained in the random coil conformation.

To evaluate the polarity of the environment and the mobility of the free radicals, hyperfine splitting constants (A_0) and the rotational correlation times (τ_c) were calculated from the simulated spectra. The value of A_0 is sensitive to the polarity of the medium in which the radical resides. A larger value is typically observed in more polar environments

owing to the greater electron density in nitrogen or the pseudoionic structure (Deo & Somasundaran, 2002). For x-DSA samples, A_0 is 14.42 ± 0.01 G in DMSO and 15.65 ± 0.01 G in water, and for PTMIO samples, A_0 is 14.37 ± 0.01 G in DMSO and 15.50 ± 0.01 G in water. The higher A_0 value of probe in water than that in DMSO indicated that the nitroxide radicals were surrounded by a more polar medium. The presence of amylose in a physical mixture did not affect the A_0 of probes in either solvent, which implies that the N-O• is not in close association with amylose.

The change in the mobility of the probe was evaluated from the rotational correlation time, τ_c, (Table 1). Theoretically, a smaller value of τ_c (shorter time) means faster molecular motion. The calculated values were in agreement with that reported previously for similar molecules (Ahlin, Kristl, Pečar, Štrancar, & Šentjurc, 2003; Yucel et al., 2012). The rotational correlation times of the aliphatic probes were slightly, but significantly, higher than that of PTMIO since they are larger molecules. The higher rotational correlation time of 5-DSA than that of 16-DSA can be attributed to the bent confirmation of 5-DSA (Dzikovski & Livshits, 2003). Contrary to that reported by Wasserman & Le Meste (2000), where x-DSA was shown to be strongly adsorbed to potato starch granules at room temperature in starch-water systems, there was no significant difference in rotational correlation time of the probes in the presence and absence of amylose. The difference is probably due to the much higher solubility of amylose and their random coil conformation in DMSO. In addition, Wasserman & Le Meste (2000) suggested that surface proteins on starch granules might also contribute to the adsorption of aliphatic spin probes. Yet, the surface proteins had been removed during the amylose purification process.

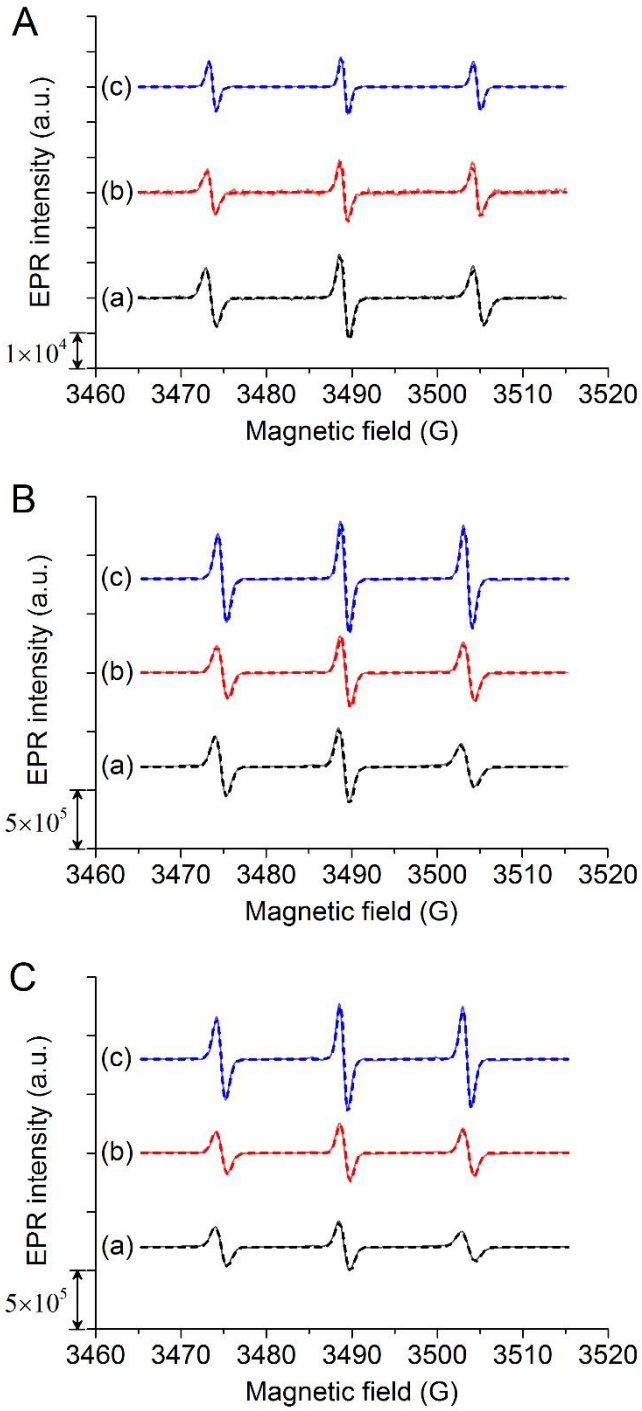

281

282 Fig. 4. EPR spectra of solutions of spin probes (a) 5-DSA, (b) 16-DSA, and (c) PTMIO (100
283 μM) in (A) water, (B) DMSO, and (C) DMSO with amylose as physical mixtures at room
284 temperature (25 °C). Dash lines show the simulated spectra over the raw data. The signal
285 amplitude of PTMIO in water was divided by 50 to rescale with those of aliphatic spin probes.

Table 1. Rotational correlation time (τ_c) of solutions of probes (5-DSA, 16-DSA, and PTMIO), amylose-probe physical mixtures (PM), and amylose-probe inclusion complexes (IC) in DMSO and water (T = 20 °C). Different letters show significant difference ($p < 0.05$) in a column, while Roman numerals show the significant difference ($p < 0.05$) in a row.

Sample		$\tau_{DMSO} \times 10^{11}$ (s)	$\tau_{water} \times 10^{11}$
Probe	5-DSA	$5.61 \pm 0.26^{a,I}$	$5.07 \pm 0.19^{a,I}$
	16-DSA	$3.38 \pm 0.11^{b,I}$	$3.08 \pm 0.13^{b,I}$
	PTMIO	$1.91 \pm 0.10^{c,I}$	$1.29 \pm 0.11^{c,II}$
PM	5-DSA	$6.12 \pm 0.09^{ad,I}$	$5.19 \pm 0.15^{a,II}$
	16-DSA	$3.48 \pm 0.34^{b,I}$	$3.14 \pm 0.10^{b,I}$
	PTMIO	$1.93 \pm 0.16^{c,I}$	$1.31 \pm 0.09^{c,II}$
IC	5-DSA	6.43 ± 0.28^{d}	—
	16-DSA	3.68 ± 0.19^{b}	

As aforementioned, the two aliphatic spin-probes, 5- and 16-DSA, were evidenced to form inclusion complexes with amylose, whereas the aromatic PTMIO was not able to form inclusion complex. The EPR spectra of amylose-probe inclusion complexes in DMSO and water (supernatant extraction) are shown in Fig. 5. Since DMSO is a good solvent for amylose, the spin probes included in amylose molecules were released into DMSO upon the dissociation of amylose helices. The PTMIO signal is low in both DMSO and water because it was not included within the helices and thus was lost during sample preparation (i.e., ethanol washing step). On the contrary, the release of x-DSA from the inclusion complexes into DMSO suggests that they were effectively encapsulated within the amylose helices. Since water is not a good solvent for amylose inclusion complex at room temperature, there was no spin-probe released into the supernatant when amylose-5-DSA inclusion complex was added to water. However, in the case of 16-DSA, a very small fraction of the spin-probe partitioned into water, suggesting that some 16-DSA molecules associated with amylose in a manner making it susceptible to water extraction. Although the inclusion complex is largely insoluble in water, the amorphous region is more susceptible to water and a portion of amylose may be dissolved, which is also known as “amylose leaching” when starch is

dispersed in water. Yet this portion is small, because DSC data showed considerable amount of 16-DSA included in the inclusion complex that can only be released when heated to their dissociation temperature around 101 °C. The water partitioning of 16-DSA from its inclusion complex could be attributed to the possible localization of a small fraction of 16-DSA in amorphous amylose phase. A parallel behavior was also observed for slow tumbling spectra (Fig. 6), which will be discussed later.

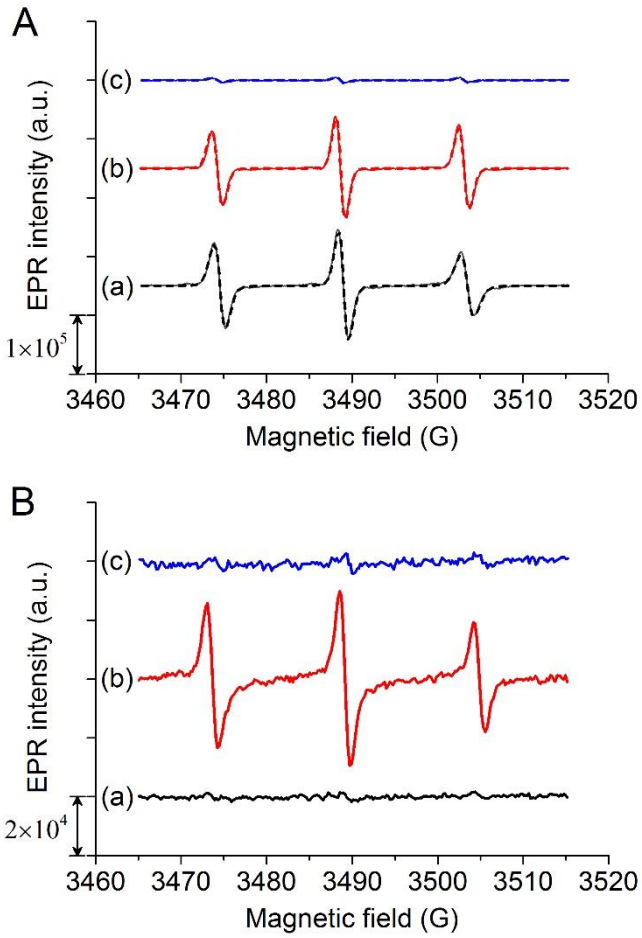

Fig. 5. Solution spectra of amylose inclusion complexes with spin probes (a) 5-DSA, (b) 16-DSA, and (c) PTMIO in (A) DMSO and (B) water (supernatant) at room temperature. Dash lines show the simulated spectra over the raw data.

In addition to the solution spectra discussed above, slow spectra were also measured and analyzed for the dry inclusion complexes and hydrated inclusion complexes in water (Fig. 6).

Slow spectra of amylose without guest compounds and amylose-PTMIO samples were not examined. Calculated parameters are presented in Table 2. The spectra are close to the powder-like spectra of spin probe immobilization by starches observed in previous studies (Biliaderis & Vaughan, 1987; Nolan et al., 1986; Wasserman & Le Meste, 2000). EPR spectra of both 5-DSA and 16-DSA in inclusion complexes showed increased mobility with hydration. This observation suggests that the doxyl ring moiety is outside the helix and thus exposed to the aqueous environment. In a similar manner to the solution spectra, the 16-DSA was more mobile than 5-DSA in the inclusion complex, by showing a superimposed spectrum of two components with fast and slow motions (Fig. 6d). The motion of 16-DSA after hydration was largely heterogenous. The change in $A_{\parallel}$ (from 33.44 G to 30.51 G) upon hydration is quite different than that in $A_{\perp}$ (from 6.75 G to 12.69 G) (i.e., the extent of changes in the motion about the parallel vs. the perpendicular to the axis of rotation). In other words, the tumbling motion of the probe is relatively more restricted along the length of the molecule than short-axis (i.e., more free in the small radius of rotation). This observation suggested that upon hydration the binding of 16-DSA to amylose is not as strong as 5-DSA. It is possible that some 16-DSA molecules were immobilized extra-helically in a few random places, especially in the amorphous region. This is consistent with the solution spectra which showed the partition of a small amount into the water. Indeed, Biais et al. suggested that the guest molecules can be trapped intrahelically and interhelically in the crystalline layer, and some guest molecules can also be associated with amylose molecules in the amorphous region (Biais, Le Bail, Robert, Pontoire, & Buléon, 2006). The τ_c values for the included probes were much greater than those of the free-moving probes (i.e., in DMSO) suggesting that they largely remain within the complex even after hydration.

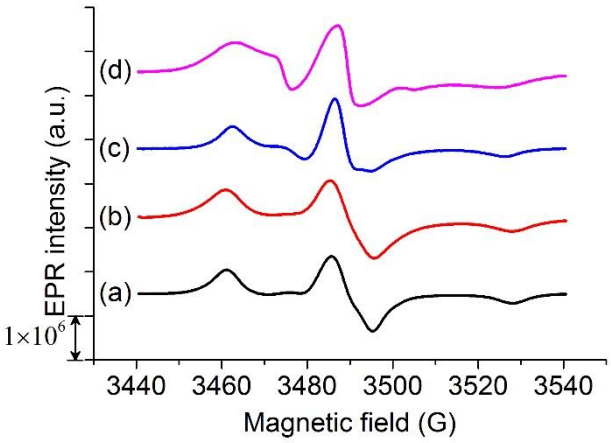

341

342 **Fig. 6.** EPR spectra of dry inclusion complex samples (*i.e.*, rigid limit) of (a) amylose-5-DSA
343 and (b) amylose-16-DSA and hydrated inclusion complex samples (c) amylose-5-DSA and
344 (d) amylose-16-DSA.

345 **Table 2.** The order parameter (S), and the rotational correlation time (τ_c) for hydrated
346 inclusion complex as calculated from Equations 1 and 2. Parameters (*e.g.*, A_{max}) for the rigid
347 spectra (*i.e.*, in dry powders) measured experimentally.

Sample	A_{max}(G)	S	τ_c (ns)
Amylose-5-DSA inclusion complex	33.38 ± 0.06	0.954 ± 0.035	35.36 ± 1.09
Amylose-16-DSA inclusion complex	33.44 ± 0.05	0.912 ± 0.066	14.77 ± 0.68

348

349 **4. Conclusion**

350 In conclusion, amylose inclusion complexes with aliphatic spin probes, including 5- and
351 16-DSA, as guest molecules were prepared and confirmed by complementary XRD, DSC, and
352 FTIR techniques. The spin probes, and their physical mixtures and inclusion complexes with
353 amylose were additionally studied by EPR spectroscopy, which provides information on the
354 molecular dynamics and local polarity of spin probes. Physical mixture of the spin probes and
355 amylose in DMSO increased the microviscosity of the spin probes but did not foster binding

356 due to the solubility and conformation of amylose. Since the amylose inclusion complex is
357 soluble in DMSO, the spin probes were released and detected by EPR. It again confirmed that
358 PTMIO was not able to form inclusion complex with amylose because it was not detectable
359 when the sample was dissolved in DMSO. The amylose inclusion complex added into water
360 could not be dissolved, therefore, both solution spectra of the supernatant and slow spectra of
361 the hydrated sample were recorded. Both spectra suggested higher mobility of 16-DSA than 5-
362 DSA, which could be attributed to at least a portion of 16-DSA molecules that were not tightly
363 encapsulated in the crystalline amylose helices but resided in the amorphous region that was
364 more susceptible to hydration. In addition to x-DSA, there may be other spin probes as
365 appropriate guest molecules that could provide more information on the the microstructure and
366 microenvironment of amylose inclusion complexes. EPR spectroscopy represents as an
367 emerging tool for studying these host-guest supramolecular structures and other starch-based
368 systems.

369 **Acknowledgment**

370 This work was funded by the USDA National Institute for Food and Agriculture, National
371 Competitive Grants Program, National Research Initiative Program 71.1 FY 2007 as grant #
372 2007-35503-18392.

References

Ahlin, P., Kristl, J., Pečar, S., Štrancar, J., & Šentjurc, M. (2003). The effect of lipophilicity of spin-labeled compounds on their distribution in solid lipid nanoparticle dispersions studied by electron paramagnetic resonance. *Journal of Pharmaceutical Sciences*, *92*(1), 58–66.

Avramiotis, S., Cazianis, C. T., & Xenakis, A. (2000). Membrane spin-probe studies in lecithin and bis (2-ethylhexyl) sulfosuccinate sodium salt water-in-oil microemulsions. *Trends in Colloid and Interface Science XIV*, *115*, 196–200.

Barbon, A., Zoleo, A., Brustolon, M., Comotti, A., & Sozzani, P. (2008). One-dimensional clusters of 16-doxyl-stearate radicals in organic nanochannels as studied by electron paramagnetic resonance (EPR). *Inorganica Chimica Acta*, *361*(14), 4122–4128.

Bardelang, D., Rockenbauer, A., Jicsinszky, L., Finet, J.-P., Karoui, H., Lambert, S., … Tordo, P. (2006). Nitroxide bound β-cyclodextrin: Is there an inclusion complex? *The Journal of Organic Chemistry*, *71*(20), 7657–7667.

Beghein, N., Rouxhet, L., Dinguizli, M., Brewster, M. E., Ariën, A., Préat, V., … Gallez, B. (2007). Characterization of self-assembling copolymers in aqueous solutions using Electron Paramagnetic Resonance and Fluorescence spectroscopy. *Journal of Controlled Release*, *117*(2), 196–203.

Biais, B., Le Bail, P., Robert, P., Pontoire, B., & Buléon, A. (2006). Structural and stoichiometric studies of complexes between aroma compounds and amylose. Polymorphic transitions and quantification in amorphous and crystalline areas. *Carbohydrate Polymers*, *66*(3), 306–315.

Biliaderis, C. G., Page, C. M., & Maurice, T. J. (1986). Non-equilibrium melting of amylose-V complexes. *Carbohydrate Polymers*, *6*(4), 269–288.

Biliaderis, C. G., Page, C. M., Slade, L., & Sirett, R. R. (1985). Thermal behavior of amylose-lipid complexes. *Carbohydrate Polymers*, *5*(5), 367–389.

Biliaderis, C. G., & Vaughan, D. J. (1987). Electron spin resonance studies of starch-water-probe interactions. *Carbohydrate Polymers*, *7*(1), 51–70.

Bluhm, T. L., & Zugenmaier, P. (1981). Detailed structure of the Vh-amylose-iodine complex: a linear polyiodine chain. *Carbohydrate Research*, *89*(1), 1–10.

Bratt, P. J., & Kevan, L. (1993). Electron spin resonance line-shape analysis of x-doxylstearic acid spin probes in dihexadecyl phosphate vesicles and effects of cholesterol addition. *The Journal of Physical Chemistry*, *97*(28), 7371–7374.

Brigati, G., Franchi, P., Lucarini, M., Pedulli, G. F., & Valgimigli, L. (2002). The EPR study of dialkyl nitroxides as probes to investigate the exchange of solutes between micellar and water phases. *Research on Chemical Intermediates*, *28*(2–3), 131–141.

Brisson, J., Chanzy, H., & Winter, W. T. (1991). The crystal and molecular structure of VH amylose by electron diffraction analysis. *International Journal of Biological Macromolecules*, *13*(1), 31–39.

Carlson, T., Larsson, K., Dinh-Nguyen, N., & Krog, N. (1979). A study of the amylose-monoglyceride complex by Raman spectroscopy. *Starch-Stärke*, *31*(7), 222–224.

Conde-Petit, B., Escher, F., & Nuessli, J. (2006). Structural features of starch-flavor complexation in food model systems. *Trends in Food Science & Technology*, *17*(5), 227–235.

Deo, N., & Somasundaran, P. (2002). Electron spin resonance study of phosphatidyl choline vesicles using 5-doxyl stearic acid. *Colloids and Surfaces B: Biointerfaces*, *25*(3), 225–232.

Deo, N., Somasundaran, P., Subramanyan, K., & Ananthapadmanabhan, K. P. (2002). Electron paramagnetic resonance study of the structure of lipid bilayers in the presence

of sodium dodecyl sulfate. *Journal of Colloid and Interface Science*, *256*(1), 100–105.
Dzikovski, B. G., & Livshits, V. A. (2003). EPR spin probe study of molecular ordering and dynamics in monolayers at oil/water interfaces. *Physical Chemistry Chemical Physics*, *5*(23), 5271–5278.
Eliasson, A.-C., & Wahlgren, M. (2004). Starch-lipid interactions and their relevance in food products. *Starch in Food: Structure, Function, and Applications. Woodhead, Cambridge*, 441–454.
Freed, J. H. (1976). Theory of slowly tumbling ESR spectra for nitroxides. In L. J. Berliner (Ed.), *Spin Labeling: Theory and Applications* (pp. 53–132). New York: Academic Press, Inc.
Gaffney, B. J. (1976). Appendix IV: Practical considerations for the calculation of order parameters for fatty acid or phospholipid spin labels in membranes. In L. J. Berliner (Ed.), *Spin Labeling: Theory and Applications* (pp. 567–571). New York: Academic Press, Inc.
Garay, A. S., & Rodrigues, D. E. (2008). Effects of the inclusion of the spin label 10-doxyl-stearic acid on the structure and dynamics of model bilayers in water: stearic acid and stearic acid/cholesterol (50: 20). *The Journal of Physical Chemistry B*, *112*(6), 1657–1670.
Godet, M. C., Bouchet, B., Colonna, P., Gallant, D. J., & Buleon, A. (1996). Crystalline amylose-fatty acid complexes: morphology and crystal thickness. *Journal of Food Science*, *61*(6), 1196–1201.
Godet, M. C., Buleon, A., Tran, V., & Colonna, P. (1993). Structural features of fatty acid-amylose complexes. *Carbohydrate Polymers*, *21*(2), 91–95.
Griffith, O. H., & Jost, P. C. (1976). Lipid spin labels and biological membranes. In L. J. Berliner (Ed.), *Spin Labeling: Theory and Applications* (pp. 454–523). New York: Academic Press, Inc.
Immel, S., & Lichtenthaler, F. W. (2000). The hydrophobic topographies of amylose and its blue iodine complex. *Starch - Stärke*, *52*(1), 1–8.
Karkalas, J., Ma, S., Morrison, W. R., & Pethrick, R. A. (1995). Some factors determining the thermal properties of amylose inclusion complexes with fatty acids. *Carbohydrate Research*, *268*(2), 233–247.
Kong, L., & Ziegler, G. R. (2014a). Formation of starch-guest inclusion complexes in electrospun starch fibers. *Food Hydrocolloids*, *38*(0), 211–219.
Kong, L., & Ziegler, G. R. (2014b). Molecular encapsulation of ascorbyl palmitate in preformed V-type starch and amylose. *Carbohydrate Polymers*, *111*(13), 256–263.
Kristl, J., Volk, B., Gašperlin, M., Šentjurc, M., & Jurkovič, P. (2003). Effect of colloidal carriers on ascorbyl palmitate stability. *European Journal of Pharmaceutical Sciences*, *19*(4), 181–189.
Lay Ma, U., Floros, J. D., & Ziegler, G. R. (2011). Formation of inclusion complexes of starch with fatty acid esters of bioactive compounds. *Carbohydrate Polymers*, *83*(4), 1869–1878.
Le Bail, P., Bizot, H., Ollivon, M., Keller, G., Bourgaux, C., & Buléon, A. (1999). Monitoring the crystallization of amylose–lipid complexes during maize starch melting by synchrotron x-ray diffraction. *Biopolymers*, *50*(1), 99–110.
Lebail, P., Buleon, A., Shiftan, D., & Marchessault, R. H. (2000). Mobility of lipid in complexes of amylose–fatty acids by deuterium and 13C solid state NMR. *Carbohydrate Polymers*, *43*(4), 317–326.
Lesmes, U., Cohen, S. H., Shener, Y., & Shimoni, E. (2009). Effects of long chain fatty acid unsaturation on the structure and controlled release properties of amylose complexes. *Food Hydrocolloids*, *23*(3), 667–675.

Lorentz, C., Pencreac'h, G., Soultani-Vigneron, S., Rondeau-Mouro, C., de Carvalho, M., Pontoire, B., … Le Bail, P. (2012). Coupling lipophilization and amylose complexation to encapsulate chlorogenic acid. *Carbohydrate Polymers*, *90*(1), 152–158.

Mezzina, E., Cruciani, F., Pedulli, G. F., & Lucarini, M. (2007). Nitroxide radicals as probes for exploring the binding properties of the cucurbit [7] uril host. *Chemistry-A European Journal*, *13*(25), 7223–7233.

Nakagawa, K. (2009). EPR investigations of spin-probe dynamics in aqueous dispersions of a nonionic amphiphilic compound. *Journal of the American Oil Chemists' Society*, *86*(1), 1–17.

Nolan, N. L., Faubion, J. M., & Hoseney, R. C. (1986). An electron spin resonance study of native and gelantinized starch systems. *Cereal Chemistry*, *63*(4), 287–291.

Pearce, L. E., Davis, E. A., Gordon, J., & Miller, W. G. (1985). Application of electron spin resonance techniques to model starch systems. *Food Structure*, *4*(1), 10.

Pearce, L. E., Davis, E. A., Gordon, J., & Miller, W. G. (1987). Stearic acid-starch interactions as measured by electron spin resonance. *Cereal Chemistry*, *64*(3), 154–157.

Putseys, J. A., Gommes, C. J., Van Puyvelde, P., Delcour, J. A., & Goderis, B. (2011). < i> In situ</i> SAXS under shear unveils the gelation of aqueous starch suspensions and the impact of added amylose–lipid complexes. *Carbohydrate Polymers*, *84*(3), 1141–1150.

Stauffer, C. E. (1995). *Functional additives for bakery foods*. New York: Springer.

Štrancar, J., Šentjurc, M., & Schara, M. (2000). Fast and accurate characterization of biological membranes by EPR spectral simulations of nitroxides. *Journal of Magnetic Resonance*, *142*(2), 254–265.

Tapanapunnitikul, O., Chaiseri, S., Peterson, D. G., & Thompson, D. B. (2007). Water solubility of flavor compounds influences formation of flavor inclusion complexes from dispersed high-amylose maize starch. *Journal of Agricultural and Food Chemistry*, *56*(1), 220–226.

Tufvesson, F., Wahlgren, M., & Eliasson, A. (2003). Formation of amylose-lipid complexes and effects of temperature treatment. Part 2. fatty acids. *Starch-Stärke*, *55*(3–4), 138–149.

Wasserman, L. A., & Le Meste, M. (2000). Influence of water on potato starch–lipid interactions. An electron spin resonance (ESR) probe study. *Journal of the Science of Food and Agriculture*, *80*(11), 1608–1616.

Whittam, M. A., Orford, P. D., Ring, S. G., Clark, S. A., Parker, M. L., Cairns, P., & Miles, M. J. (1989). Aqueous dissolution of crystalline and amorphous amylose-alcohol complexes. *International Journal of Biological Macromolecules*, *11*(6), 339–344.

Windle, J. J. (1985). An ESR spin probe study of potato starch gelatinization. *Starch-Stärke*, *37*(4), 121–125.

Wu, F., & Gaffney, B. J. (2006). Dynamic behavior of fatty acid spin labels within a binding site of soybean lipoxygenase-1. *Biochemistry*, *45*(41), 12510–12518.

Yucel, U., Elias, R. J., & Coupland, J. N. (2012). Solute distribution and stability in emulsion-based delivery systems: An EPR study. *Journal of Colloid and Interface Science*, *377*(1), 105–113.